International Journal of Environmental Science and Technology (2022) 19:4615–4626
https://doi.org/10.1007/s13762-021-03464-2

ORIGINAL PAPER

Fabrication and evaluation of nanofiltration membrane coated with amino-functionalized graphene oxide for highly efficient heavy metal removal

S. Lari[1] · S. A. M. Parsa[1] · S. Akbari[2] · D. Emadzadeh[3,4] · W. J. Lau[5]

Received: 2 April 2021 / Revised: 3 June 2021 / Accepted: 8 June 2021 / Published online: 2 July 2021

Abstract

In this study, two different methods were used to introduce functionalized graphene oxide (GO) onto the surface of nanofiltration (NF) membrane to improve its performance for heavy metal removal. The first method was based on coating in which the surface of NF membrane was coated with cross-linked GO, while the second method was introducing GO into monomer solution during interfacial polymerization. The efficiency of different methods was then compared by characterizing membrane physiochemical properties, as well as separation performance. With regard to performances, the water flux of TFN-i2 membrane (with GOs incorporated into thin layer) was reported to be 95 L/m^2 h compared to 75 L/m^2 h found in the TFN-c2 membrane (with GOs coated on the surface) at 8 bar. Both modified membranes exhibited higher water flux than the control membrane without GO incorporation (40 L/m^2 h). Although the water flux of TFN-c2 membrane was lower, it achieved higher cobalt removal (97%) than that of TFN-i2 membrane (73%) due to its higher negative surface charge that improved separation via the Donnan exclusion effect.

Editorial responsibility: Maryam Shabani.

✉ D. Emadzadeh
d.emadzadeh@iaug.ir

[1] Department of Chemical Engineering, Yasooj Branch, Islamic Azad University, Yasooj, Iran

[2] Department of Textile Engineering Department, Amirkabir University of Technology (Polytechnic Tehran), Tehran, Iran

[3] Department of Chemical Engineering, Gachsaran Branch, Islamic Azad University, Gachsaran, Iran

[4] Department of Chemical and Biological Engineering, University of Ottawa, 161 Louis Pasteur St, Ottawa, ON K1N 6N5, Canada

[5] Advanced Membrane Technology Research Centre (AMTEC), Universiti Teknologi Malaysia, 81310 Skudai, Johor, Malaysia

Graphic abstract

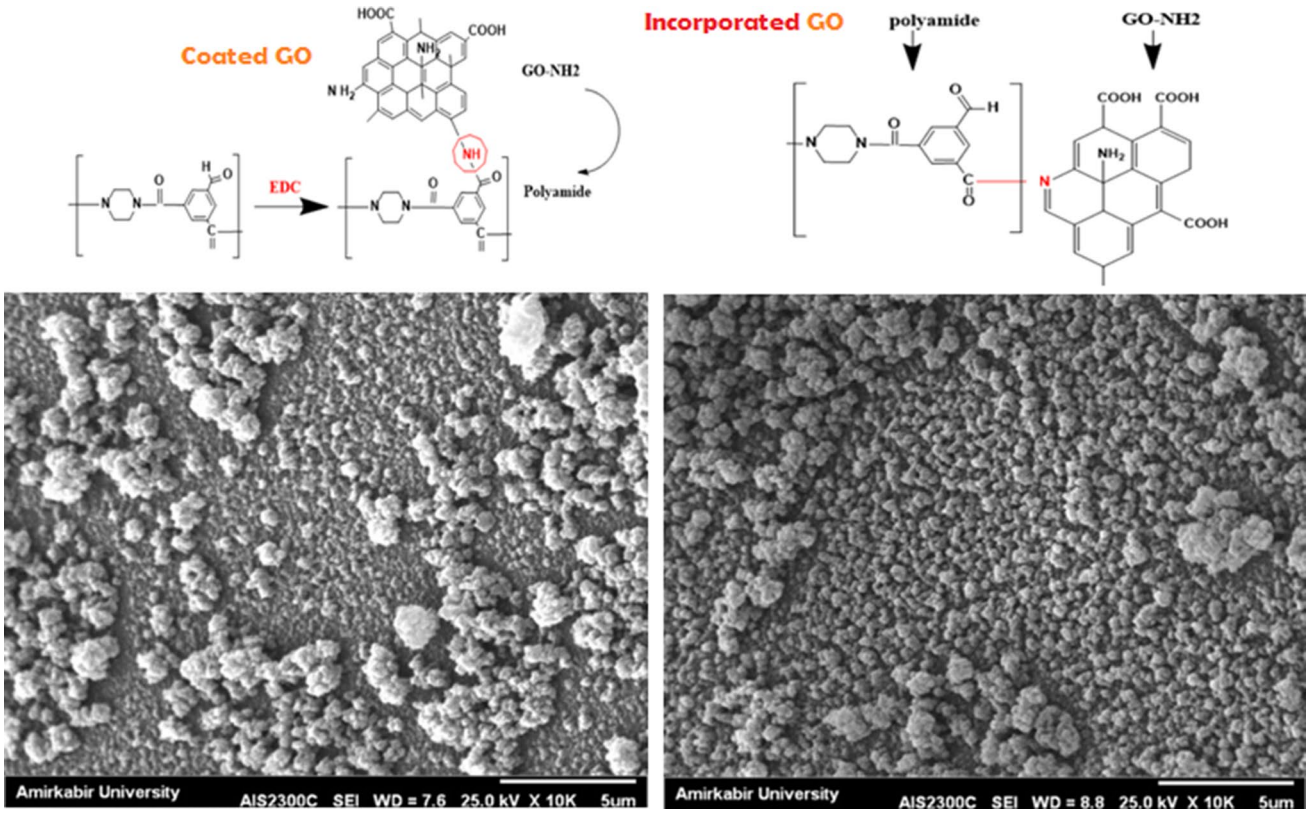

Keywords Graphene oxide · Surface modification · Thin-film nanocomposite membrane · Nanofiltration · Heavy metal

Abbreviations

CA	Contact angle
NF	Nanofiltration
GO	Graphene oxide
IP	Interfacial polymerization
TFN	Thin-film nanocomposite
RO	Reverse osmosis
UF	Ultrafiltration
TFC	Thin-film composite
PA	Polyamide
NPs	Nanoparticles
TiO2	Titanium dioxide
SiO2	Silicon dioxide
APTES	3-Aminopropyltriethoxsylane
PSF	Polysulfone
NMP	N-methyle-2-pyrrolidone
PVP	Polyvinylpyrrolidone
TMC	Trimesoyl chloride
PIP	Piperazine
EDC	(1-Ethyl-3-(3-dimethylaminopropyl) carbodiimide hydrochloride
DI	Deionized water
GO-NH2	Modified GO
FTIR	Fourier transform infrared spectroscopy
SEM	Scanning electron microscopy

Introduction

Insufficient clean water supply coupled with severe water pollution are the main problems faced by many countries in the world (Montgomery and Elimelech 2007; Pendergast and Hoek 2011). One of the problems causing water pollution is the discharge of heavy metals by industrial activities such as mining and petrochemical process (Csavina et al. 2012). These heavy metals are highly toxic and stable and cannot be easily metabolized. They can accumulate in living organisms and enter to the food chain, causing great threats to the ecosystem, as well as human (Celis et al. 2000; Özcan et al. 2018).

Accumulation of low concentration of heavy metals in human body can cause serious health problems such as endocrine illnesses, cardiac diseases, chronic respiratory diseases (asthma, pneumonia and fibrosis), nervous system

disorders and even cancer (Finch et al. 2011; Fu and Wang 2011). Thus, removal of heavy metals from wastewater has become increasingly important in recent years (Farokhi et al. 2021; Gheimasi et al. 2021).

In comparison with other heavy metal's elimination methods, membrane filtration process is more appealing due to its high separation efficiency, no phase change requirement, small footprint and environmentally friendly (Escobar and Van der Bruggen 2011; Qdais and Moussa 2004). Membrane-based techniques in particular nanofiltration (NF) which is based on combined sieving and Donnan exclusion effect are currently drawing a lot of research interest in water purification. This pressure-driven membrane is different with reverse osmosis (RO) and ultrafiltration (UF) membranes in terms of membrane pore size and charge properties (Bowen et al. 1997).

Typically, the NF membrane is in the structure of thin-film composite (TFC) that is composed of an ultrathin polyamide (PA) layer reinforced by a highly permeable polymeric support. Numerous methods are available to develop ultrathin barrier layer of TFC NF membrane. These include the most popular interfacial polymerization, grafting, dip-coating, electron beam irradiation and plasma-initiated polymerization (Lau et al. 2012).

Different nanoparticles such as titanium dioxide (TiO_2) (Emadzadeh et al. 2014), silicon dioxide (SiO_2), silver, carbon nanotubes (CNTs) and zeolites have been used to modify PA layer of NF membrane which lead to the formation of new type of membrane known as thin-film nanocomposite (TFN) (Emadzadeh et al. 2015; Lau et al. 2015). Embedding nanoparticles within PA layer is one of the most significant achievements for improving membrane performance for water applications. Currently, nanocomposite membranes are extensively used in NF because of their potential for high selectivity and permeability, thermal and mechanical properties, electrochemical and anti-swelling performance, and anti-fouling properties. However, the use of nanoparticles in modifying PA layer also leads to another problem, i.e., surface defects in selective layer as the result of nanoparticles agglomeration and poor bonding/compatibility between NPs and polymer (Buonomenna 2013; Lau et al. 2015; Pendergast and Hoek 2011).

To address the abovementioned issues, surface modification of nanoparticles is a simple and effective method to increase their dispersion in monomers solutions during interfacial polymerization process and to enhance their compatibility with organic materials (Vatanpour et al. 2014). Chemically modified graphene (a carbon atomic hexagonal) has received great attention due to its excellent electrical, mechanical and thermal properties (De Silva et al. 2017; Yin et al. 2013). Graphene oxide (GO) contains a range of reactive oxygen functional agents such as carboxyl (–COOH), hydroxyl (–OH) and epoxy (–C–O–C) that make it potentially suitable for absorbent in environmental applications. (Chen et al. 2015; Zhao et al. 2016). Thus, modification of GO using other functional groups is required. Moreover, functionalization could improve the properties of GO and increase its capacity to adsorb heavy metal ions from wastewater (Gul et al. 2016). Although GO has an effective adsorption capacity over metal ions, it does not have the selective adsorption property of heavy metals, therefore, several metal cations can be adsorbed on the surface of GO from their mixtures. As a result, competitive adsorption occurs and the percentage of adsorption is dependent on the differences between affinity and the metal ions toward GO (Sitko et al. 2013).

In this study, the self-synthesized GO was first modified using (3-aminopropyl) triethoxysilane (APTES). Then, the functionalized GO was introduced onto the membrane surface using two different techniques. The first method was to deposit the GO on the membrane surface via coating and the second method was to incorporate GO into PA layer during interfacial polymerization (IP). All resulting membranes were then characterized using different analytical instruments before they were evaluated with respect to water flux and cobalt removal rate.

Materials and methods

Materials and reagents

To fabricate membrane substrate, polysulfone (PSF) (Solvay Advanced Polymers with 22,400 g/mol), N-methyle-2-pyrrolidone (NMP) (99.5%) and polyvinylpyrrolidone (PVP K30, mol wt ~ 40,000, Sigma-Aldrich) were used to form the polymeric dope solution followed by casting. Trimesoyl chloride (TMC, 98%), piperazine (PIP, 99%) and n-hexane were purchased from the Merck Company and used to develop selective layer atop substate. In addition, graphite particles (average particle size smaller than 100 nm), 3-aminopropyltriethoxylane (99%), potassium permanganate ($KMnO_4$), ethanol (C_2H_6O, 95%), sulfuric acid (H_2SO_4, 98%), phosphoric acid (H_3PO_4, 85%) and chloride (37%) were obtained from Merck and were used to synthesize GO followed by modification. (1-ethyl-3-(3-dimethylaminopropyl) carbodiimide hydrochloride (EDC, 98%, Sigma-Aldrich) was used as a cross-linker. Cobalt(II) nitrate hexahydrate (Sigma-Aldrich) was selected as a heavy metal sample for the preparation of feed solution. Deionized water (DI) was prepared using MilliQ water purification system.

Graphene oxide (GO) synthesis

GO nanoparticles were prepared using graphite powder by the modified Hummers' method (Marcano et al. 2010). In brief, 3 g of graphite was added into a mixture of H_2SO_4 (98%) and H_3PO_4 in a ratio of 9:1 followed by 2-h mixing. Then, 18 g of $KMnO_4$ was added to the mixture and stirred (using magnetic stirrer) at 50 °C for 24 h to obtain a homogeneous solution. External heating is required for this step as it is essential for the reaction. After 24 h, the solution was cooled followed by lowering its temperature to approximately 0 °C by adding ice water into the mixture. To complete the oxidation process, 3-mL hydrogen peroxide was added and the mixture was placed in an ice bath to maintain its temperature. It was then washed with DI water, HCl and C_2H_6OH, respectively. Finally, the GO nanoparticles were placed in the vacuum oven to dry completely.

Chemical modification of GO

The chemical modification of GO nanoparticles is very important in order to create a new functional group and increase its reactivity with the PA layer of the composite membrane during the interfacial polymerization process. In this study, modifications have been applied to improve the adsorption capacity of GO using APTES—a silane coupling agent with two amino groups in one molecule. The amino group ($–NH_2$) could be then attached onto the GO nanoparticles (Hong et al. 2013; Li et al. 2013). To modify GO, firstly, 300 mg of GO was dispersed in a 150-mL ethanol followed by sonication for 30 min at ambient temperature. Then, 2.3 mL of APTES substance was added to the prepared mixture in the presence of N_2 gas. The mixture was then stirred at room temperature under reflux for 24 h. Finally, the solid phase was centrifuged for 10 min at 4000 rpm and washed eight times with ethanol and water to eliminate residual APTES. The final product obtained ($GO–NH_2$) was then dried at 100 °C in a vacuum oven to release bubbles.

Preparation of polysulfone substrate

In the current research, the casting solution was prepared by dissolving 16.5 wt% of PSF in 82.5 wt% NMP. Then, 1% (w/v) of PVP solution was added and stirred on magnetic stirrer for 24 h. The solution was then poured onto a glass frame using special molding film and immersed it immediately in a water-coagulating bath at room temperature. Membranes were then developed within few seconds due to phase separation. Finally, the fabricated membranes were washed to remove residual solvents with water and sorted in a DI water bath until they were examined.

Preparation of composite membranes

TFC membrane was synthesized using interfacial polymerization. In detail, PIP and TMC were dissolved in deionized water and hexane, respectively. To obtain the permeable polyamide layer from TFC membranes, the synthesized PSF substrate was placed on a glass plate and fixed with a rubber gasket. Then, 2% PIP solution was added to the substrate for 2 min. After that, 0.15 wt% of TMC solution was added to first monomer for 1 min. To eliminate unreacted PIP and TMC from the surface of TFC membrane, the prepared membrane was rinsed with n-hexane. Then, the fabricated membrane was placed in oven at 60° C for 5 min as post-treatment.

In the present study, to modify the surface of PA layer, modified GO (i.e., $GO–NH_2$) was added on the TFC membrane surface using two different methods. In the first method, GO nanoparticles were coated atop membrane using EDC activator which thereafter called as TFN-c1, TFN-c2 or TFN-c3 depending on amount of nanoparticles added (0.01, 0.05 and 0.1%). The carboxyl groups of PA were first converted into amine-reactive esters by contacting the membrane with EDC.

In the second method, functionalized GO was incorporated into TMC as chloride monomer to fabricate PA layer during IP. The synthesized membranes based on nanoparticles concentration ranging from 0.01, 0.05 and 0.1% called as TFN-i1, TFN-i2 or TFN-i3.

Evaluation of membrane performance

In the present study, the performance of the synthesized TFN membranes and TFC membranes with various concentrations of GO in different pH values (3, 7 and 8) was evaluated. Feed solution composed of 100 ppm cobalt ions was made by dissolving the appropriate weight of cobalt nitrate hexahydrate ($Co(NO_3)_2$ 6 H_2O) in DI water. Separation characteristics of the membrane such as permeability and rejection rate were measured using a cross-flow system as shown in Fig. 1.

The laboratory-scale system includes a tank, flow meter, pump, valves, pressure indicator and a membrane cell. The membrane effective surface area in the cell was 23 cm^2, and the pH value was measured using a pH meter (HQ411d, HACH, USA). Prior to the evaluation of membranes in the cross-flow system, the membranes were first compacted by placing them in the cell membrane and then pressed at 8 bar at 0.5 L/min flow rate. In addition, a 2-L tank containing aqueous solution of Co^{2+} ions at concentration of 100 ppm was supplied as a feed solution. The performance of TFC and TFN membranes in the constant state was evaluated by measuring the solute volumetric flux and rejection

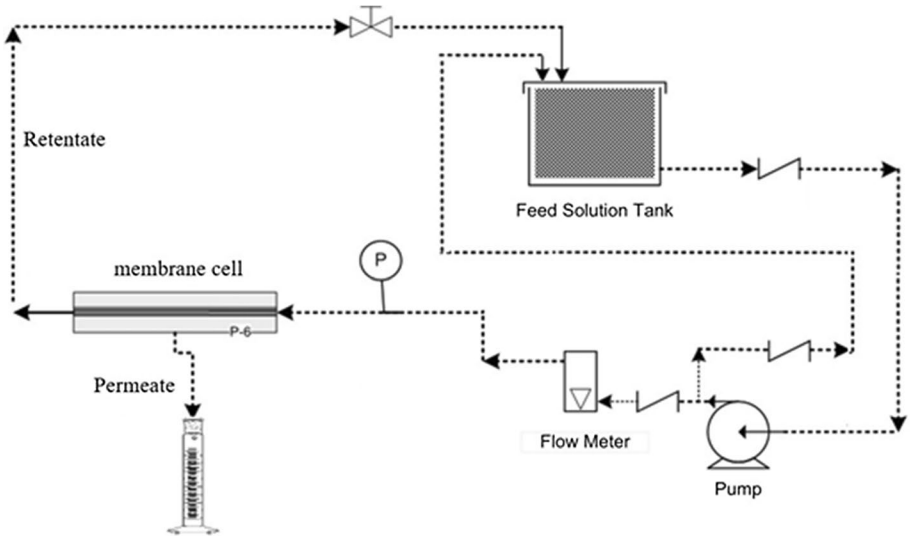

Fig. 1 Schematic diagram of cross-flow NF filtration unit

of passing solution through the system under steady-state condition (8 bar and flow rate of 2 L/min) at room temperature. In this experiment, the permeate volume flux (J_v, $Lm^{-2}\ h^{-1}$) of membranes is evaluated using Eq. (1).

$$J_v = \frac{V}{(A)(\Delta T)} \tag{1}$$

where V is volumetric water volume (L), A is effective membrane surface area (m^2) and T is filtration time (h). In addition, the heavy metal rejection (R, %) of membrane was calculated based on the feed (C_p) and permeate concentration (C_f) (mg/L) using the following equation.

$$R = \left(1 - \frac{C_p}{C_f}\right) \times 100 \tag{2}$$

Membrane characterization

Fourier transform infrared spectroscopy (FTIR, EQUINOX55) was used to record the changes of functional groups and elements in the GO nanoparticles, as well as flat sheet TFC and TFN membranes based on Omnic™ Software. The membrane was dried at 60 °C for 24 h before being analyzed. The membrane surface was randomly chosen and scanned at a rate of 16 scans per second to investigate the functional groups presented in different samples. The contact angle between the dry surface of the membrane and the DI water droplet was measured using the Angle Contact Meter (CA-VP, Kyowa) made by the Japanese company Interface Science. The cross section and surface morphology of the membrane were monitored by scanning electron microscopy (SEM, VEGAIII, TESCAN). The samples were first washed with ethanol and were frozen and fractured in liquid nitrogen for cross-sectional photography. The samples were then sputtered with a layer of gold followed by visualization under SEM. The surface charging properties of fabricated membranes were measured as a function of pH using a zeta potential analyzer (Particle Metrix ZetaView).

Results and discussion

FTIR analysis of nanomaterials and membranes

Infrared spectroscopy analysis was performed in order to examine the functional groups on the surface of GO (Fig. 2) and membranes (Fig. 3). The graphite sample includes two intensive peaks at a wave numbers of 3420 cm^{-1} and

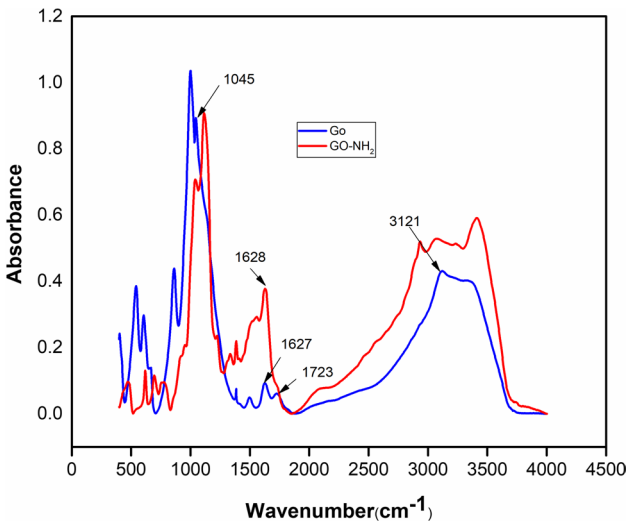

Fig. 2 FTIR spectra of GO and APTES-modified GO

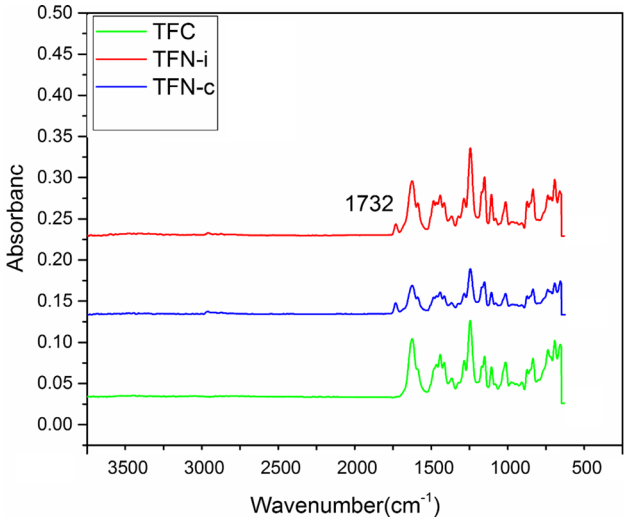

Fig. 3 FTIR spectra of TFC and TFN membranes

1641 cm^{-1} which indicate the tensile hydroxyl group and the skeletal vibration of graphite, respectively, due to the absorption of water and the C=C aromatic ring stretching. Meanwhile, the peak at 1723 cm^{-1} is assigned to C=O bonding of the GO skeleton. The detection of two other peaks at 1047 cm^{-1} and 1250 cm^{-1} indicates the presence of a bending C-O bond and oxygen functional group in the GO sample, respectively. Concurrently, the transition of C=C aromatic peak from 1637 cm^{-1} in graphite to 1627 cm^{-1} in GO demonstrates the binding of some functional groups to the aromatic ring after oxidation. A broad peak is also seen at around 3121 cm^{-1}, and it is mainly due to the presence of the hydroxyl group in the original GO structure. This is where a broad peak is assigned to stretching vibration of O–H bond and confirms the presence of hydroxyl functional group. However, this peak intensity was greatly reduced after APTES modification due to reduction of hydroxyl groups (–OH) and reaction between OH and silane (Si–O) groups. A new peak appeared at 1628 cm^{-1} is corresponded to C=N group, confirming the successful APTES functionalization (Xiao et al. 2016).

GO shows characteristic peaks at 3121, 1723, 1384 and 1041 cm^{-1} which are belonged to hydroxyl groups, carbonyl groups and C–O vibration of epoxy groups, respectively. After APTES is used to functionalize GO, the peak belonging to carbonyl group is converted to amide group. As a result, peak at 1723 cm^{-1} is omitted and a strong peak (1628 cm^{-1}) corresponding to amino functional groups is detected.

Figure 3 illustrates the FTIR spectra of TFC (control) and different TFN membranes. For TFC membrane, the specific wave number of 1145 cm^{-1} (symmetric O=S=O stretching), 1300 cm^{-1} (asymmetric O=S=O stretching), 1250 cm^{-1} (asymmetric C–O–C stretching), 1500 cm^{-1} (CH3-C–CH3 stretching) and 1405 cm^{-1} (C=C aromatic ring stretching) is corresponded to the specific functional groups of substrate made of PSf. Peaks are clearly seen at 1732 cm^{-1} and 1626 cm^{-1} in the composite and nanocomposite membranes, respectively, which overlap with the amide peaks in both membranes. However, the peak at 1732 cm^{-1} which only appeared in the TFN membranes might indicate the reaction between NH_2 groups of modified GO and -COOH of PA layer.

Membrane morphology

Figure 4 compares the micrographs of the TFC and TFN membranes made of two different methods. Figure 4a reveals a TFC membrane, which contains a relatively smooth surface that is corresponded to a thin and compacted PA formed atop the PSF substrate. The considerable increase in the concentration of GO on the surface of the TFC membrane alters the membrane structure and surface morphology changes (Fig. 4b) which might be due to increasing hydrophilicity. Thus, it creates more sites in the PA layer and increases the membrane surface area. However, Fig. 4c demonstrates the surface structure modified by coating. As can be seen, its surface is rougher compared to the TFC membrane and this could be due to the accumulation of nanoparticles on the membrane surface.

Zeta potential

Figure 5 shows the zeta potential of TFC and TFN membranes at various pH value ranging from 3 to 8. It can be observed that by increasing the pH, the negative charge on the surface of the TFC and TFN membranes is increased accordingly. Compared to the TFC membrane, the negative charge property of TFN membrane is reported to be higher. The zeta potential for TFN-c2 membranes showed a more negative surface charge than the TFC and TFN-i2 membrane at all pH range due to the presence of more carboxylic groups. In addition, the greatest negative zeta potential of TFN-c2 membrane can also be attributed to the presence of abundance of nanoparticles on its surface by coating (Kaleekkal et al. 2017; Mukherjee et al. 2016).

Performance evaluation of the TFC and TFN membranes

For the first method (coating method), the TFN-c membrane was fabricated by coating its surface with GO. Since there are some inactive functional groups such as carboxylic acid (–COOH) on the surface of the polyamide layer, these groups can be changed to active sites for bonding to the nanoparticles. Thus, intermediate compound such as EDC can be used to provide more reactive sites on the

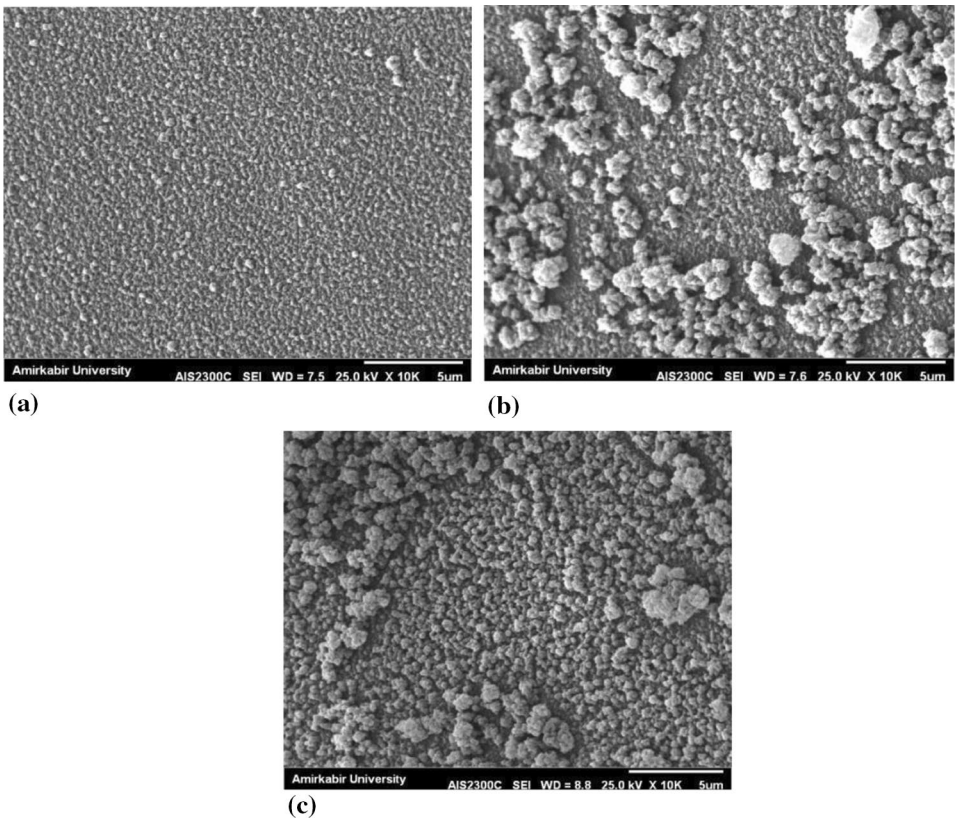

Fig. 4 SEM micrographs of **a** TFC, **b** TFN-i2 and **c** TFN-c2 membrane

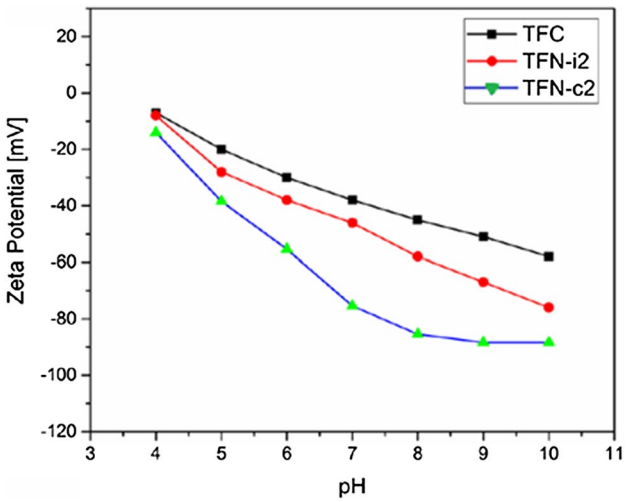

Fig. 5 Zeta potential of TFC, TFN-i2 and TFN-c2 membrane at different pH values

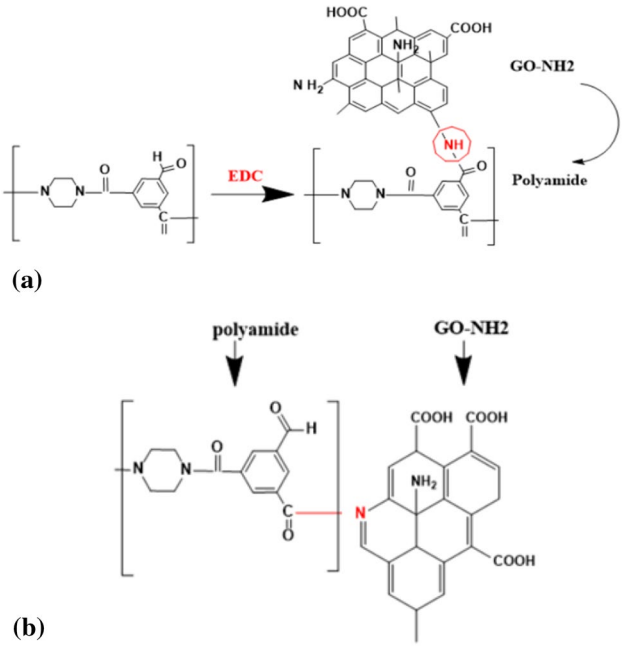

Fig. 6 Possible interaction between modified GO and PA layer, **a** via coating method and **b** IP method

surface of the PA membrane before depositing GO onto its surface. Therefore, GO is firstly modified using APTES. It is followed by converting the hydroxyl (OH) group to the active NH_2. Then, EDC, which is an intermediate component, activates the membrane surface and converts –COOH functional group to COO-, aiming to increase its reactivity.

When modified GO (GO–NH_2) is added to TMC aqueous solution during interfacial polymerization process, it might compete with PIP and react with TMC to form an amide

Table 1 Pure water flux and contact angle of prepared membrane by coating and IP method

Membrane	PWF (L/m^2 h)	CA (°)	Membrane	PWF (L/m^2 h)	CA(°)
TFC	42	64.7	TFC	42	64.7
TFN-c1	60	47.2	TFN-i1	63	62
TFN-c2	82	26.6	TFN-i2	99	60
TFN-c3	71	18.5	TFN-i3	125	58

bond which eventually affects the PA cross-linking degree. The GO–NH_2 nanoparticles react with the COO^- group via NH_2 as illustrated in Fig. 6a. Meanwhile, for the second method, the TFN-i2 membrane was fabricated by incorporating GO during interfacial polymerization process as shown in Fig. 6b as explained in methodology section.

The performance of TFC and TFN membranes was evaluated using 100 ppm Co solution as a feed solution. Table 1 reveals the water flux and water contact angle (CA) for TFC membrane and TFN membranes. The contact angle of membrane decreased upon the addition of nanoparticles, and subsequently, water flux was also increased due to improved hydrophilicity. According to the data, the CA of the nanocomposite membrane for both modified methods was significantly reduced, indicating that the GO-NH_2 functionalization provides a strong hydrophilic polar amide functional on the surface of the membranes. Thus, the CA in coated method was reduced from 64.7° for the TFC membrane to 18.5° for the TFN membrane at different concentrations from zero for TFC to 0.01, 0.05, 0.1 for TFN membranes, respectively. It was also reduced in the IP method from 64.7° to 58°. Therefore, in both modification methods, adding different concentrations of modified GO nanoparticles on the PA surface improved the hydrophilic properties of nanocomposite membrane compared with TFC membrane. This increase in membrane hydrophilicity could be attributed to the existence of abundant hydrophilic (-OH) functional groups of nanoparticles and the hydrophilic nature of GO nanoparticles which have also been reported in similar studies (Rezaee et al. 2015; Yu et al. 2006).

Owing to high hydrophilic properties of modified membrane made of coating method, these membranes are supposed to have greater water flux than the modified membranes made of IP method. However, the results are opposite as the water flux of TFN-i membranes is found to be higher than those of TFN-c membranes. Adding modified GO nanoparticles to the surface of the TFC membrane using coating method and also simultaneously with the formation of a thin layer and IP improved their flux and permeability compared with the TFC membrane. In addition, the flux improvement could be explained by various reasons. First, GO contains large number of hydroxyl (-OH) and carboxylic (-COOH) groups which can give unique properties to the membrane, change its morphology and directly affect flux and membrane permeability. As a result, the presence of PA layer and the distribution of hydrophilic functional groups can accelerate and facilitate the movement of water molecules through the membrane. On the other hand, because of the natural structure of nanoparticles, placing them on the membrane surface and also changing its morphology cause the formation of new channels for filtration and passing water molecules through the membrane (Wu et al. 2013; Yin et al. 2012; Zhao et al. 2013).

Figure 7 compares water flux of membranes made of two different methods. As can be seen, the water flux of TFN membranes is better compared to the typical TFC membrane. By increasing the nanoparticles from zero to 0.05%, the percentage of water flux increment is found to be greater for the TFN-i membrane compared to the TFN-c membrane and this may be due to the changes in membrane structure and the channels existed in the selective layer. For the membranes made of coating method, increasing the nanoparticles concentration on the membrane surface created an additional layer with more nanoparticles which subsequently reduced the membrane cross-flow compared with the membrane made of IP method. Moreover, the decrease in the flux for the coated membrane with the highest nanoparticles (TFN-c3) can be attributed to the severe accumulation of nanoparticles in the membrane structure that blocks the membrane pores. Similar results are obtained from other nanoparticles such as silica and ordered mesoporous carbon (OMC) that negatively affected the membrane water flux due to the high concentration of

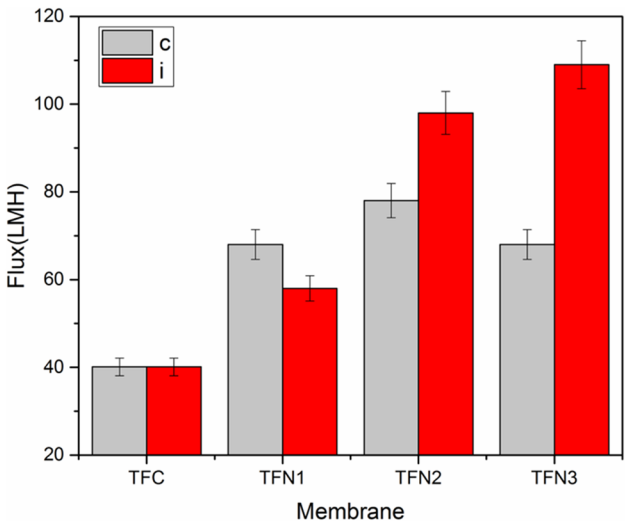

Fig. 7 Comparison of water flux for TFC and TFN membranes with different modification methods (TFN-c and TFN-i)

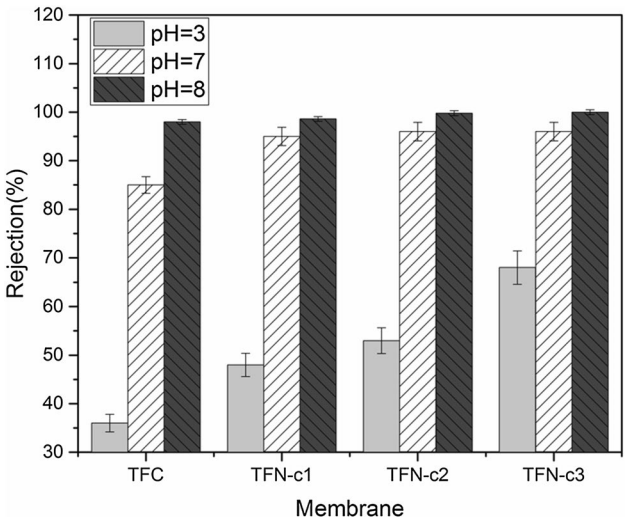

Fig. 8 Effect of pH on rejection performance of TFC and TFN membranes by coating method in various pH values

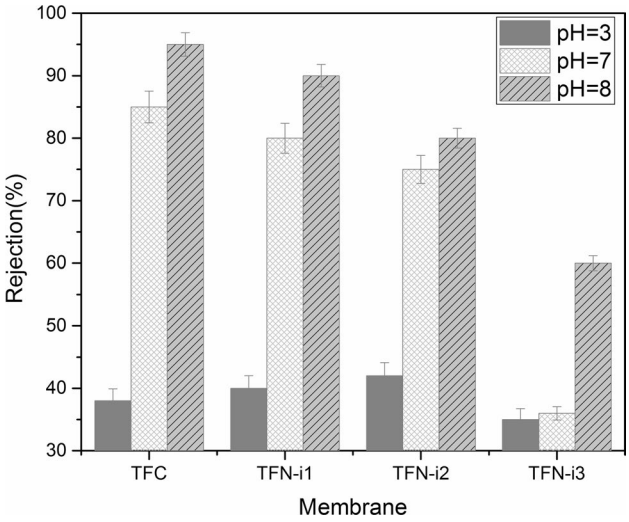

Fig. 9 Effect of pH on rejection performance of TFC membrane and TFN membranes at different pH values

nanoparticles and their accumulation in the thin-film layer (Kim and Deng 2011; Yin et al. 2012).

Figure 8 presents the rejection trend of TFC membrane and TFN-c membranes. As shown, in the high pH value (basic), the rate of heavy metal rejection of all membranes was higher compared to the low pH value (acidic). However, these changes were not seen at pH 7. On the other hand, with the increase in the concentration of nanoparticles, the rejection rate at all basic pH is reported to increase, which may be due to the higher negatively charge property of TFN membranes that tends to reject NO^{3-} of $Co(NO_3)_2$ through the Donnan exclusion effect. Furthermore, the addition of modified GO nanoparticles to the surface of PA layer is found to increase the rejection rate of TFC membrane at pH ranging from 3 to 7. However, TFN-c membranes with various concentrations of nanoparticles did not show any change at pH 7 because CO^{+2} at pH greater than 7 tends to precipitate as $CO(OH)_2$ and could remain almost constant at pH > 8.

The addition of GO nanoparticles to the membrane surface could increase the cobalt ion rejection because of the higher negatively charge of the resultant TFN membranes. Additionally, pH value is one of the most important parameters in the removal of heavy metals during NF process due to its effect on the surface charge, ionization, speciation and binding site of the adsorbent (Kamani et al. 2016; Shah and Murthy 2013). Based on the results obtained from zeta potential, pH variation is predominantly attributed to the presence of polar groups including hydroxyl (–OH)- and carboxylic (–COOH)-modified GO on the membrane surface, which provides prerequisites for the removal of heavy metals on the membrane surface (Rezaee et al. 2015). Therefore, the increase in pH from 3 to 8 results in a higher negative charge of the membrane due to the increase in –OH group which causes the adsorption of heavy metal ions at the surface of the TFC. The adsorption of heavy metal is also related to the electrostatic interaction at the surface of membrane, which affects not only the water flux but also the rejection. In addition, the membrane charge can also differ significantly due to the equilibrium between the surface groups of the membrane. Studies have suggested that the mechanisms of adsorption of heavy metal ions on GO surface are attributed to electrostatic attraction, ion exchange and surface complexation (Cao and Li 2014; Li et al. 2015). Electrostatic attraction between positively charged heavy metal ions and negatively charged GO provides available active sites on the membrane surface for cobalt ions absorption.

Increasing the pH (reduction in hydrogen ion concentration) results in increased dissociation of carboxyl and hydroxyl groups in GO nanoparticles membranes. Consequently, the density of negative charge on GO at pH ≥ 7 was higher than pH ≤ 7, which revealed that the gravity force of GO at pH ≥ 7 would be stronger than that acidic and neutral conditions (Zhang et al. 2017).

According to Fig. 9, the rejection rate of heavy metal in the basic pH was higher than that of acidic pH which could be observed in all membranes with different percentages of nanoparticles in IP method. It is also clear that with increase in nanoparticles, the rejection rate in all pH was decreased due to changes in the surface of membrane as discussed before. In fact, these results support that the addition of modified GO to the PA membrane using IP method decreased the effective reaction between GO and membrane surface due to the inactivation of active site

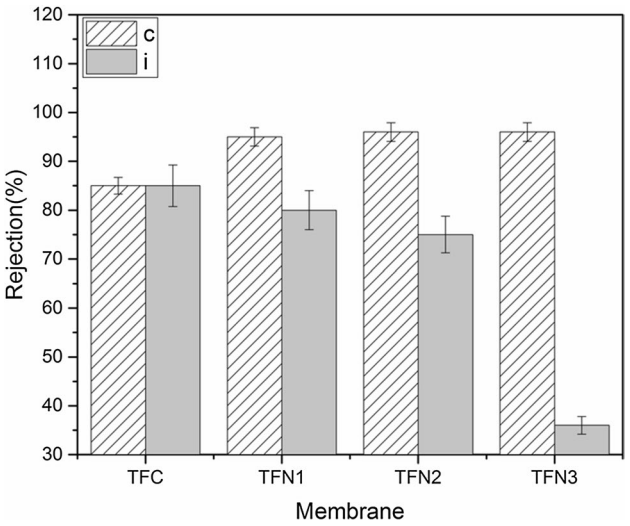

Fig. 10 Rejection comparison of TFC and TFN membranes at pH 7

of polar groups including –OH and –COOH on the PA surface.

Figure 10 compares the cobalt metal removal by two types of membranes with different GO loading at pH 7. The rejection sequence was governed by three mechanisms, i.e., Donnan exclusion, size exclusion and adsorption. The surface charges of TFC, TFN-i2 and TFN-c2 membranes at pH 7 were −38.32 mV, −46.80 mV and −75.20 mV, respectively. At pH 7, when the $Co(NO_3)_2$ was used as feed solutions, the negatively charged membranes tend to reject NO^{3-} through the Donnan exclusion effect. As a result, the counter ions of Co also got rejected to preserve the electroneutrality of the solution around the membrane. This trend for TFN-c2 membrane is far more obvious which might be due to its higher negatively charge available on the PA surface. However, the reason for the decrease in the heavy metal rejection by IP method may be due to the lower effective interaction rates between GO and the membrane surface. Additionally, modified GO membranes provided various active sites to interact with metal ions. Thus, –OH and –COOH groups can interact with metal ions on the membrane surface. For this reason, the removal of ions by GO was increased because of increased active sites (Kamani et al. 2016; Shah and Murthy 2013).

Conclusion

In this study, novel PA TFN membranes were fabricated in the presence of modified GO via IP and coating method. The FTIR analysis confirmed the successful modification of GO by APTES, as well as presence of GO in the TFN membranes. In addition, the SEM micrographs revealed the changes in the surface morphology of membranes made of different methods. With regard to performances, the water flux of TFC membrane was increased from 40 to 75 L/m^2 h in the TFN-c2 membrane. By comparing with TFC and TFN-c2 membrane, the TFN-i2 membrane achieved much higher water flux, recording 95 L/m^2 h. On the other hand, cobalt removal was decreased from 85 to 73% for TFN-i2 while this result was improved from 85 to 97% for TFN-c2. In fact, unreacted COOH groups of PA layer which activated by EDC would react with NH_2 groups of modified GO, thus the amount of nanoparticles on the surface of PA may increase significantly negative surface charge that improved separation via the Donnan exclusion effect. Moreover, the effect of pH demonstrated that for all membranes, cobalt could be significantly removed in alkaline environment. However, in neutral condition, the membranes made of coating method showed better results compared to the membranes made of IP method for cobalt removal. This is due to its higher negative surface charge that improved separation via the Donnan exclusion effect.

Acknowledgements This research was partially supported by Department of Chemical Engineering, Yasooj Branch, Islamic Azad University, Yasooj, Iran. We have to express our appreciation to the Membrane Science and Technology Research Center (MSRTC), Gachsaran Branch, Islamic Azad University, for sharing their laboratory facilities with us during the course of this research.

Declarations

Conflict of interest The authors whose names are listed in this manuscript certify that they have NO affiliations with or involvement in any organization or entity with any financial interest (such as honoraria; educational grants; participation in speakers' bureaus; membership, employment, consultancies, stock ownership, or other equity interest; and expert testimony or patent-licensing arrangements), or non-financial interest (such as personal or professional relationships, affiliations, knowledge or beliefs) in the subject matter or materials discussed in this manuscript.

References

Bowen WR, Mohammad AW, Hilal N (1997) Characterisation of nanofiltration membranes for predictive purposes—use of salts, uncharged solutes and atomic force microscopy. J Membr Sci 126(1):91–105

Buonomenna M (2013) Nano-enhanced reverse osmosis membranes. Desalination 314:73–88

Cao Y, Li X (2014) Adsorption of graphene for the removal of inorganic pollutants in water purification: a review. Adsorption 20(5–6):713–727

Celis R, Hermosin MC, Cornejo J (2000) Heavy metal adsorption by functionalized clays. Environ Sci Technol 34(21):4593–4599

Chen M-L, Sun Y, Huo C-B, Liu C, Wang J-H (2015) Akaganeite decorated graphene oxide composite for arsenic adsorption/removal and its proconcentration at ultra-trace level. Chemosphere 130:52–58

Csavina J, Field J, Taylor MP, Gao S, Landázuri A, Betterton EA, Sáez AE (2012) A review on the importance of metals and

metalloids in atmospheric dust and aerosol from mining operations. Sci Total Environ 433:58–73
De Silva K, Huang H-H, Joshi R, Yoshimura M (2017) Chemical reduction of graphene oxide using green reductants. Carbon 119:190–199
Emadzadeh D, Lau W, Rahbari-Sisakht M, Daneshfar A, Ghanbari M, Mayahi A, Matsuura T, Ismail A (2015) A novel thin film nanocomposite reverse osmosis membrane with superior anti-organic fouling affinity for water desalination. Desalination 368:106–113
Emadzadeh D, Lau WJ, Matsuura T, Rahbari-Sisakht M, Ismail AF (2014) A novel thin film composite forward osmosis membrane prepared from PSf–TiO2 nanocomposite substrate for water desalination. Chem Eng J 237:70–80
Escobar I, Van der Bruggen B (2011) Modern applications in membrane science and technology. ACS Publications
Farokhi K, Cheraghi M, Sobhan Ardakani S, Lorestani B, Emadzadeh D (2021) Incorporation of modified cellulose nanocrystals to polyamide nanofiltration membrane for efficient removal of Cr (III) and Pb (II) ions from aqueous solutions. Int J Environ Analyt Chem 1–14
Finch N, Syme H, Elliott J (2011) Association of urinary cadmium excretion with feline hypertension. Veterinary Record
Fu F, Wang Q (2011) Removal of heavy metal ions from wastewaters: a review. J Environ Manag 92(3):407–418
Gheimasi MHM, Lorestani B, Sadr MK, Cheraghi M, Emadzadeh D (2021) Synthesis of novel hybrid NF/FO nanocomposite membrane by incorporating black TiO 2 nanoparticles for highly efficient heavy metals removal. Int J Environ Res 15(3):475–485
Gul K, Sohni S, Waqar M, Ahmad F, Norulaini NN, AK, M.O. (2016) Functionalization of magnetic chitosan with graphene oxide for removal of cationic and anionic dyes from aqueous solution. Carbohyd Polym 152:520–531
Hong S-M, Kim SH, Lee KB (2013) Adsorption of carbon dioxide on 3-aminopropyl-triethoxysilane modified graphite oxide. Energy Fuels 27(6):3358–3363
Kaleekkal NJ, Thanigaivelan A, Rana D, Mohan D (2017) Studies on carboxylated graphene oxide incorporated polyetherimide mixed matrix ultrafiltration membranes. Mater Chem Phys 186:146–158
Kamani H, Nasseri S, Khoobi M, Nodehi RN, Mahvi AH (2016) Sonocatalytic degradation of humic acid by N-doped TiO 2 nano-particle in aqueous solution. J Environ Health Sci Eng 14(1):3
Kim E-S, Deng B (2011) Fabrication of polyamide thin-film nanocomposite (PA-TFN) membrane with hydrophilized ordered mesoporous carbon (H-OMC) for water purifications. J Membr Sci 375(1):46–54
Lau W, Gray S, Matsuura T, Emadzadeh D, Chen JP, Ismail A (2015) A review on polyamide thin film nanocomposite (TFN) membranes: History, applications, challenges and approaches. Water Res 80:306–324
Lau W, Ismail A, Misdan N, Kassim M (2012) A recent progress in thin film composite membrane: a review. Desalination 287:190–199
Li F, Jiang X, Zhao J, Zhang S (2015) Graphene oxide: a promising nanomaterial for energy and environmental applications. Nano Energy 16:488–515
Li Z, Wang R, Young RJ, Deng L, Yang F, Hao L, Jiao W, Liu W (2013) Control of the functionality of graphene oxide for its application in epoxy nanocomposites. Polymer 54(23):6437–6446
Marcano DC, Kosynkin DV, Berlin JM, Sinitskii A, Sun Z, Slesarev A, Alemany LB, Lu W, Tour JM (2010) Improved synthesis of graphene oxide. ACS Nano 4(8):4806–4814
Montgomery MA, Elimelech M (2007) Water and sanitation in developing countries: including health in the equation. ACS Publications
Mukherjee R, Bhunia P, De S (2016) Impact of graphene oxide on removal of heavy metals using mixed matrix membrane. Chem Eng J 292:284–297
Özcan S, Çelebi H, Özcan Z (2018) Removal of heavy metals from simulated water by using eggshell powder. Desalin Water Treat 127:75–82
Pendergast MM, Hoek EM (2011) A review of water treatment membrane nanotechnologies. Energy Environ Sci 4(6):1946–1971
Qdais HA, Moussa H (2004) Removal of heavy metals from wastewater by membrane processes: a comparative study. Desalination 164(2):105–110
Rezaee R, Nasseri S, Mahvi AH, Nabizadeh R, Mousavi SA, Rashidi A, Jafari A, Nazmara S (2015) Fabrication and characterization of a polysulfone-graphene oxide nanocomposite membrane for arsenate rejection from water. J Environ Health Sci Eng 13(1):61
Shah P, Murthy C (2013) Studies on the porosity control of MWCNT/polysulfone composite membrane and its effect on metal removal. J Membr Sci 437:90–98
Sitko R, Turek E, Zawisza B, Malicka E, Talik E, Heimann J, Gagor A, Feist B, Wrzalik R (2013) Adsorption of divalent metal ions from aqueous solutions using graphene oxide. Dalton Trans 42(16):5682–5689
Vatanpour V, Esmaeili M, Farahani MHDA (2014) Fouling reduction and retention increment of polyethersulfone nanofiltration membranes embedded by amine-functionalized multi-walled carbon nanotubes. J Membr Sci 466:70–81

Wu H, Tang B, Wu P (2013) Optimizing polyamide thin film composite membrane covalently bonded with modified mesoporous silica nanoparticles. J Membr Sci 428:341–348

Xiao W, Yan B, Zeng H, Liu Q (2016) Dendrimer functionalized graphene oxide for selenium removal. Carbon 105:655–664

Yin J, Kim E-S, Yang J, Deng B (2012) Fabrication of a novel thin-film nanocomposite (TFN) membrane containing MCM-41 silica nanoparticles (NPs) for water purification. J Membr Sci 423:238–246

Yin J, Yang Y, Hu Z, Deng B (2013) Attachment of silver nanoparticles (AgNPs) onto thin-film composite (TFC) membranes through covalent bonding to reduce membrane biofouling. J Membr Sci 441:73–82

Yu H-Y, Xu Z-K, Yang Q, Hu M-X, Wang S-Y (2006) Improvement of the antifouling characteristics for polypropylene microporous membranes by the sequential photoinduced graft polymerization of acrylic acid. J Membr Sci 281(1–2):658–665

Zhang P, Gong J-L, Zeng G-M, Deng C-H, Yang H-C, Liu H-Y, Huan S-Y (2017) Cross-linking to prepare composite graphene oxide-framework membranes with high-flux for dyes and heavy metal ions removal. Chem Eng J 322:657–666

Zhao C, Xu X, Chen J, Yang F (2013) Effect of graphene oxide concentration on the morphologies and antifouling properties of PVDF ultrafiltration membranes. J Environ Chem Eng 1(3):349–354

Zhao D, Gao X, Wu C, Xie R, Feng S, Chen C (2016) Facile preparation of amino functionalized graphene oxide decorated with Fe3O4 nanoparticles for the adsorption of Cr (VI). Appl Surf Sci 384:1–9